2024 European Control Conference (ECC)
June 25-28, 2024. Stockholm, Sweden

Safe platooning and merging control using constructive barrier feedback

Xiao Chen[1], Zhiqi Tang[1], Karl H. Johansson[1] and Jonas Mårtensson[1]

Abstract— **This paper proposes a novel formation control design for safe platooning and merging of a group of vehicles in multi-lane road scenarios. Provided a leader vehicle is independently controlled, the objective is controlling the follower vehicles to drive in the desired lane with a constant desired distance behind the neighboring (preceding) vehicle while preventing collisions with both the neighboring vehicle and the road's edges. Inspired by the recent concept of constructive barrier feedback, the proposed controller for each follower vehicle is composed of two parts: one is the nominal controller that ensures its tracking of the neighboring vehicle; another is for collision avoidance by using divergent flow as a dissipative term, which slows down the relative velocity in the direction of the neighboring vehicle and road edges without compromising the nominal controller's performance. The key contribution of this work is that the proposed control method ensures collision-free platooning and merging control in multi-lane road scenarios with computational efficiency and systematic stability analysis. Simulation results are provided to demonstrate the effectiveness of the proposed algorithms.**

I. Introduction

In recent years, the technology of connected and automated vehicles (CAV) has experienced significant progress. The synergistic integration of reliable sensor, communication, and control technologies on CAVs enables them to form fleet-level cooperation in road operations, leading to innovative solutions for addressing various traffic challenges [1]. As pioneered by PATH project [2] in the early 2000s, vehicle platooning, defined as a train of CAVs operating with short inter-vehicle distances and synchronized speeds in a shared trip, is one important representation of cooperative driving technologies. Various studies have highlighted the potential benefits of vehicle platooning, encompassing increased road capacity, enhanced safety, improved fuel efficiency, and reductions in travel delays and road congestion [3]–[5].

Early works (e.g., [6]–[8]) have been dedicated to studying one-dimensional longitudinal motion control for a platoon of vehicles. The focus is maintaining safe inter-vehicle distances for vehicles on a single lane to drive at the same speed and to ensure string stability. In a multi-lane traffic setting, guiding vehicles into a platoon formation requires additional consideration for safe lane-changing maneuvers concerning neighboring vehicles. Additionally, vehicles must navigate within a structured road environment, requiring adaptable formation adjustments to accommodate the road's shape and robust lane-keeping mechanisms to prevent encroachment on road edges. In summary, collision avoidance in a structured road environment remains a critical open challenge for platoon formation in multi-lane road scenarios.

A majority of literature about collision avoidance focuses on designing gradient descent control laws based on constructing the potential function using geometric information on the considered topology [9]. Yet, most solutions only consider single-integrator systems due to the position feedback used for the collision avoidance effect. The work in [10] exploits potential functions for collision-free flocking of a group of double-integrator systems, and the authors in [11] apply this algorithm to a safe platoon control in a multi-lane scenario. However, restricted initial condition on both the position and velocity of the whole formation is needed for collision avoidance between agents. Recently, optimization-based controllers based on model predictive control (MPC) [12], [13] and control barrier functions (CBF) [14] have emerged as promising alternatives to guarantee safety between agents. However, their application in vehicle platooning often imposes limited considerations, such as ignoring road boundaries or focusing only on lateral or longitude controller design. For instance, a distributed MPC is employed in [12] to ensure collision-free vehicle platooning with a dedicated design of terminal constraints, however restricted in the longitudinal direction. The CBF-based control approach has been exploited for safe lane change maneuvers in [15], whereas vehicles are modeled as a simple first-order system and the constraint of limited free space on the road is ignored. It is worth noting that the use of optimization-based control approaches poses challenges in explicitly analyzing the equilibrium and convergence of the multi-robot system, in addition to potential computational complexity and feasibility issues.

Recently, Tang et al. propose in [16] a novel concept of constructive barrier feedback inspired by natural systems like insects and birds, which exploits *divergent flow* [17] to prevent collisions while effectively achieving the primary control objective. The decentralized controller proposed in [16] is designed as the sum of a nominal tracking controller and the constructive barrier feedback composed of the divergent flow in the direction of the neighboring vehicle. The constructive barrier feedback here serves as dissipative velocity feedback that slows down the relative velocity in the direction of the neighboring vehicle without compromising the nominal controller's performance. Its application to collision-free formation control under an acyclic digraph topology outperforms classical barrier function approaches and potential field methods, resulting in computationally efficient collision avoidance algorithms with systematic equilibrium analysis.

[1]Xiao Chen, Zhiqi Tang, Karl H. Johansson and Jonas Mårtensson are with the Division of Decision and Control Systems, School of Electrical Engineering and Computer Science, KTH Royal Institute of Technology, SE-10044 Stockholm, Sweden. Emails: {xiao2, ztang2, kallej, jonas1}@kth.se

In this paper, the constructive barrier feedback approach in [16] is adopted to design a safe platoon formation control in a multi-lane road setting while considering limited free space within road boundaries. The focus is to design control input for the center point of the front axle of the car, which is modeled as a double integrator. Then, the control input is transferred to the control design of a kinematic bicycle model as in [18]. By assuming the leader vehicle is independently controlled, for each follower vehicle, the proposed controller is designed as the sum of two parts: one is the nominal controller that ensures its tracking of the neighboring vehicle; another is for collision avoidance by using divergent flow as a dissipative term. Under the proposed controller, i) the follower vehicles remain within a safe distance to both the neighboring vehicle and road edges at all times as long as the initial condition is within the safe distance; ii) the tracking error in terms of position and velocity converges asymptotically to zero. The proposed method is simple and elegant in design, and its effectiveness is validated in simulations for both merging and platoon formation scenarios.

The remaining sections of this paper are structured as follows. In Section II, we provide the necessary preliminaries on the constructive barrier feedback approach. In Section III, we state the vehicle model and its transformation together with the problem formulation of this paper. Section IV outlines the detailed formulation of the proposed controller and theoretical results. In Section VI, we conduct numerical evaluations of the method and compare it with a nominal formation control without the collision avoidance component. Finally, in Section VII, we provide concluding remarks on our work.

II. Preliminary

Consider a system of n $(n \geq 2)$ connected agents in the platooning scenarios. The underlying interaction topology can be modeled as a digraph (directed graph) $\mathcal{G} := (\mathcal{V}, \mathcal{E})$, where $\mathcal{V} = \{1, 2, \ldots, n\}$ is the set of vertices and $\mathcal{E} \subseteq \mathcal{V} \times \mathcal{V}$ is the set of directed edges. The set of neighbors of agent i is denoted by $\mathcal{N}_i := \{j \in \mathcal{V} | (i, j) \in \mathcal{E}\}$. To provide clarity on the graph topology used in this work, we make the following assumption:

Assumption 1: The topology $\mathcal{G}$ is fixed and described by an acyclic digraph with a single directed spanning tree, as shown in Fig. 1. Without loss of generality, agents are numbered (or can be renumbered) such that agent 1 is the leader, i.e. $\mathcal{N}_1 = \varnothing$, all other agents $i,\ i \geq 2$ are followers whose neighboring set is $\mathcal{N}_i = \{i - 1\}$.

A. Constructive barrier feedback for collision avoidance

In this section, we will recall the concept of constructive barrier feedback proposed in [16] for collision avoidance of a leader-follower structure in which each vehicle dynamics is described as a double integrator as follows

$$\begin{cases} \dot{p}_i = v_i \\ \dot{v}_i = u_i \end{cases} \tag{1}$$

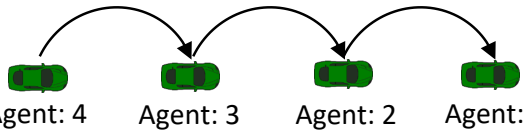

Fig. 1: Interaction topology for a 4-agent platoon formation scenario. The arrow indicates the information access for each agent i from its neighboring agent $i - 1$.

where $p_i \in \mathbb{R}^2$ is the position, $v_i \in \mathbb{R}^2$ is the velocity of each agent i, respectively, and $u_i \in \mathbb{R}^2$ is the input acceleration.

The relative position vectors between two neighboring agents i and $i - 1$ is defined as:

$$e_i := p_{i-1} - p_i,\ i \geq 2. \tag{2}$$

Similarly, $\nu_i := \dot{e}_i = v_{i-1} - v_i$ denotes the relative velocity between agent i and $i - 1$. As long as $\|e_i\| \neq 0$, one can define direction vector from i to $i - 1$ as:

$$g_i = \frac{e_i}{\|e_i\|} \in \mathbb{S}^1$$

where $\mathbb{S}^1 := \{y \in \mathbb{R}^2 : \|y\| = 1\}$ denote the 1-Sphere.

Let r be a positive constant that we term the safety distance and define

$$d_i := \|e_i\| - r = \|p_{i-1} - p_i\| - r. \tag{3}$$

A straightforward computation shows that $\dot{d}_i = g_i^\top \nu_i$.

To prevent collisions between neighboring agents, the key principle is controlling the relative velocity along the direction g_i, i.e., $\dot{d}_i = g_i^\top \nu_i$. To get an effective reactive collision avoidance without affecting the stability property of the nominal controller, feedback controller u_i is designed in [16] as:

$$u_i = u_i^n + k_o g_i f^B(\dot{d}_i, d_i),\ i \in \mathcal{V}/\{1\}, \tag{4}$$

with k_o a positive constant gain and u_i^n the nominal control input ensuring the asymptotic (or the exponential) stability of the equilibrium $(e_i - e_i^*, \nu_i - \nu_i^*) = (0, 0)$, where e_i^* and ν_i^* denote desired relative position and velocity, respectively. And

$$\phi_i := f^B(\dot{d}_i, d_i) = \frac{\dot{d}_i}{d_i} = \frac{g_i^\top \nu_i}{d_i} \tag{5}$$

a dissipative control barrier feedback slowing down the relative velocity in the direction of the neighbor without compromising the stability nature of the nominal control action. It can be obtained directly from the optical flow using visual information [19], or estimated from the measure of d_i [20].

To illustrate the obstacle avoidance principle employed in this context, let's consider a 2-agent system with agent $i - 1$ as the leader, agent i as the follower. Using the above definitions of $d = d_i$ and $\dot{d} = \dot{d}_i$, it is straightforward to verify that:

$$\ddot{d} = -k_o \frac{\dot{d}}{d} - \alpha_i(t) \tag{6}$$

with $\alpha_i(t) = -\frac{\|\pi_{g_i}\nu_i\|^2}{d+r} + g_i^\top(u_{i-1} - u_i^n)$. The barrier effect of the f^B, is announced in the following technical lemma:

Lemma 1: Given the dynamics (6) with k_o a positive gain and $\alpha_i(t)$ a continuous and bounded function. Then for any initial condition satisfying $d(0) > 0$ and $\phi(0) = \frac{\dot{d}(0)}{d(0)}$ bounded, the following assertions hold:

1) d remains positive, $\forall t \geq 0$.
2) d converges to zero as $t \to \infty$ if and only if (iff) $\lim_{t\to\infty} \int_0^\top \alpha(\tau)d\tau \to +\infty$.
3) If d converges to zero, then $\dot{d}$ is bounded and converges to zero, and $\phi(t)$ remains bounded, $\forall t \geq 0$. Furthermore, if $\alpha_i(t)$ converges to a positive constant $\alpha^0 > \epsilon > 0$, then $\frac{\dot{d}}{d} \to -\frac{\alpha^0}{k_o}$ and hence $\ddot{d}$ converges to zero.

Proof of the lemma is given in [16]. This lemma shows that $d = d_i$ will never cross zero for all times as long as the nominal controller u_i^n, the leader input u_{i-1}, and the relative velocity ν_i are continuous and bounded.

III. Vehicle Dynamics and Problem Formulation

In this paper, we will extend the use of constructive barrier feedback for safe platoon formation and merging control problems for a group of CAV in a multi-lane highway scenario, considering realistic car model and environmental constraints such as limited free space with road edges.

A. Vehicle dynamics

Each vehicle i is modeled as a kinematic bicycle model as the following:

$$\begin{bmatrix}\dot{x}_{ir}\\ \dot{y}_{ir}\\ \dot{\theta}_i\\ \dot{v}_{ir}\\ \dot{\delta}_i\end{bmatrix} = \begin{bmatrix}v_{ir}\cos(\theta_i)\\ v_{ir}\sin(\theta_i)\\ \frac{v_{ir}\tan(\delta_i)}{L_i}\\ 0\\ 0\end{bmatrix} + \begin{bmatrix}0 & 0\\ 0 & 0\\ 0 & 0\\ 1 & 0\\ 0 & 1\end{bmatrix}\begin{bmatrix}a_i\\ \omega_i\end{bmatrix} \tag{7}$$

where (x_{ir}, y_{ir}) and θ_i indicate the rear axle center position and orientation of vehicle i in the common global frame, v_{ir} is the speed measured at the rear wheel, and finally δ_i , L_i are the steering angle and wheelbase of vehicle i, respectively, as shown in Fig. 2. The control inputs of the system are the longitudinal acceleration a_i and the angular rate of the steering wheel w_i.

In this paper, we will focus on the control design of the vehicle's center of the front axle, which is modeled as a double integrator model (1). The control input of the kinematic bicycle model (7) is transferred from the control design of the double integrator model similarly in [18]. As shown in Fig. 2, the position of the front axle is presented as

$$p_i := \begin{bmatrix}x_{ih}\\ y_{ih}\end{bmatrix} = \begin{bmatrix}x_{ir} + L_i\cos(\theta_i)\\ y_{ir} + L_i\sin(\theta_i)\end{bmatrix}. \tag{8}$$

Take the time derivatives of p_i, the velocity at the front axle is denoted as

$$v_i := \begin{bmatrix}\dot{x}_{ih}\\ \dot{y}_{ih}\end{bmatrix} = \begin{bmatrix}v_{ir}\cos(\theta_i) - v_{ir}\sin(\theta_i)\tan(\delta_i)\\ v_{ir}\sin(\theta_i) + v_{ir}\cos(\theta_i)\tan(\delta_i)\end{bmatrix} \tag{9}$$

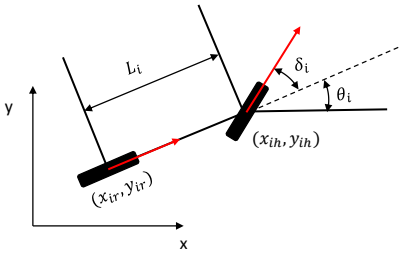

Fig. 2: Kinematic bicycle model for 2-dimensional vehicle motion.

Define the control input of the front axle's center as u_i and diffienciating again the above equation, we have

$$u_i := \begin{bmatrix}\ddot{x}_{ih}\\ \ddot{y}_{ih}\end{bmatrix} = \begin{bmatrix}-\frac{v_{ir}^2}{L}\sin(\theta_i)\tan(\delta_i) - \frac{v_{ir}^2}{L_i}\cos(\theta_i)\tan^2(\delta_i)\\ \frac{v_{ir}^2}{L_i}\cos(\theta_i)\tan(\delta_i) - \frac{v_{ir}^2}{L_i}\sin(\theta_i)\tan^2(\delta_i)\end{bmatrix} + \begin{bmatrix}\cos(\theta_i) - \sin(\theta_i)\tan(\delta_i) & -v_{ir}\sin(\theta_i)\sec^2(\delta_i)\\ \sin(\theta_i) + \cos(\theta_i)\tan(\delta_i) & v_{ir}\cos(\theta_i)\sec^2(\delta_i)\end{bmatrix}\begin{bmatrix}a_i\\ \omega_i\end{bmatrix} \tag{10}$$

The vehicle input (a_i, ω_i) can be obtained from u_i by solving (10) as follows:

$$\begin{bmatrix}a_i\\ \omega_i\end{bmatrix} = \underbrace{\begin{bmatrix}\cos(\theta_i) - \sin(\theta_i)\tan(\delta_i) & -v_{ir}\sin(\theta_i)\sec^2(\delta_i)\\ \sin(\theta_i) + \cos(\theta_i)\tan(\delta_i) & v_{ir}\cos(\theta_i)\sec^2(\delta_i)\end{bmatrix}^{-1}}_{A} \left(u_i - \begin{bmatrix}-\frac{v_{ir}^2}{L_i}\sin(\theta_i)\tan(\delta_i) - \frac{v_{ir}^2}{L_i}\cos(\theta_i)\tan^2(\delta_i)\\ \frac{v_{ir}^2}{L_i}\cos(\theta_i)\tan(\delta_i) - \frac{v_{ir}^2}{L_i}\sin(\theta_i)\tan^2(\delta_i)\end{bmatrix}\right) \tag{11}$$

which is valid as long as $\det A \neq 0$. It is straightforward to check that $\det A = v_{ir}\sec^2(\delta_i)$, so the solution to (11) exists as long as $\delta_i \neq \frac{\pi}{2}$ and $v_{ir} \neq 0$. By the physical constraint of the real car model, we have $\delta_i < \frac{\pi}{2}$. And if $v_{ir} = 0$ at a time instance, the solution of a_i still exists by solving (10), which avoids the mathematical singularity at that time instance.

B. Problem formulation

From now on, we will focus on the platoon formation control of the front axle's center of each vehicle, which is modeled as a double integrator (1).

Consider a vehicle platoon formation problem of n CAVs in a multi-lane highway scenario, as shown in Fig. 3. We adopt the following assumption about the road:

Assumption 2: The road with width $w > 0$ is placed on a flat two-dimensional plane. Two parallel straight lines define the road edges along the constant longitude direction g^* (i.e., $\dot{g}^* = 0$). The common inertial frame $\{\mathcal{I}\}$ is placed on the right road edge with axis $g^* := [1\ 0]^\top$ and $\eta^* := [0\ 1]^\top$ as can be seen in Fig. 3.

More general road segments with curvature will be considered as future works.

The desired platoon formation is defined as the group of vehicles driving on the desired lane along the longitudinal direction of the road g^* with non-zero forward velocity, as indicated in Fig. 3. More specifically, the following

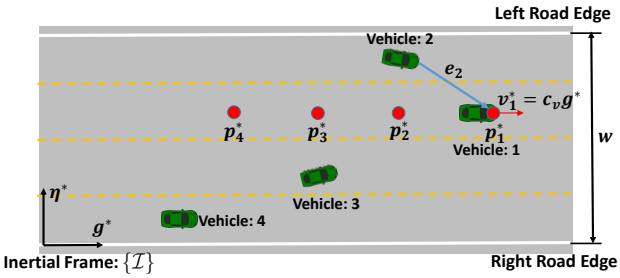

Fig. 3: Platoon formation scenario in a multi-lane highway segment at a certain time instance. The red dot indicates the desired position for each vehicle. The red arrow indicates the desired velocity for the platoon leader. The blue arrow between vehicle 2 and vehicle 1 indicates the relative position vector e_2.

assumption describes the formulation of the desired platoon formation.

Assumption 3: The leader vehicle, agent 1, is independently controlled with the formation such that $p_1 = p_1^*$ and $v_1 = v_1^* = c_v g^*$ with $c_v > 0$ the desired platoon speed. The follower vehicle, agent i, $i \geq 2$ follows its neighbor vehicle $i-1$ with desired relative position $e_i^* := p_{i-1}^* - p_i^* = c_i g^*$ and desired relative velocity $\nu_i^* := v_{i-1}^* - v_i^* = 0$ where $c_i > L_{i-1} + r > 0$ is the desired platoon distance between two neighbors and r is the safe distance between two vehicles.

The interaction topology of the platoon formation is described in Assumption 1. Since the vehicles considered in this work are homogeneous, the order of the vehicles' index is assigned according to their initial position projected to the road direction g^*.

Assumption 4: Provided ${g^*}^\top (p_i(0) - p_j(0)) \neq 0, \forall i, j \in \mathcal{V} = \{1, 2, \ldots, n\}$, the vertex set of n-vehicle systems is assigned such that ${g^*}^\top (p_{i-1}(0) - p_i(0)) > 0, \forall i \geq 2$.

The above assumption is natural in the scenarios of platoon formation, and an illustration of the index order is shown in Fig. 3.

With all the above ingredients, the problem addressed in this work is formally formulated as follows.

Problem 1: Find individual feedback control u_i for each follower vehicle $i \geq 2$ such that their front axle's center positions (p_i, v_i) converges to the desired platoon formation (p_i^*, v_i^*) while keeping a safe distance between neighbor vehicles and toward the road edges.

IV. Controller Design

Inspired by the design (4) from the work [16], the safe platoon formation controller for each follower vehicle $i \geq 2$ is proposed as two parts:

$$u_i = u_i^n + u_i^c \tag{12}$$

where u_i^n is the nominal controller for platoon formation, and u_i^c is the constructive barrier feedback design for collision avoidance against both the neighbor vehicle and road edges.

To drive the vehicle i to the desired lane while keeping a desired distance to the forward neighboring vehicle $i-1$, we decouple the control along longitude and lateral directions and design the nominal controller as

$$u_i^n = k_1 g^* {g^*}^\top (\tilde{e}_i + \nu_i) - k_2 \eta^* {\eta^*}^\top (\tilde{p}_i + \tilde{v}_i) + u_{i-1}, i \geq 2. \tag{13}$$

where k_1 and k_2 are positive gains, $\tilde{p}_i := p_i - p_i^*$, $\tilde{v}_i := v_i - v_i^*$, and $\tilde{e}_i := e_i - e_i^* = \tilde{p}_{i-1} - \tilde{p}_i$ are absolute position error, absolute velocity error and relative position error of agent i, respectively.

To prevent collision between two neighbor vehicles i and $i-1$, $d_i = \|e_i\| - r$ should be guaranteed all the time positive. Here, we explore inter-agent distance projected to the longitude direction of the road g_i^*

$$l_i := {g^*}^\top e_i - r. \tag{14}$$

Since $\|e_i\| = \sqrt{({g^*}^\top e_i)^2 + ({\eta^*}^\top e_i)^2}$, it is straightforward to verify that $l_i > 0$ implies $d_i > 0$.

Besides collision avoidance with the neighboring vehicle, all vehicles must follow the traffic rules so the road edges can not be exceeded. To avoid vehicles from crossing the two road edges, we define distance $d_i^\eta := b_i - r_\eta$ with r_η the safe distance with the road edge and b_i the minimum distance between the vehicle i and the two road edges

$$b_i := \begin{cases} {\eta^*}^\top p_i, \ {\eta^*}^\top p_i \leq \frac{w}{2}, \\ w - {\eta^*}^\top p_i, \ \text{otherwise}, \end{cases} \tag{15}$$

recall that w is the width of the road.

With the above-defined distances, the constructive barrier feedback u_i^c is designed as

$$u_i^c = k_3 g^* \phi_i^l - k_4 a_i(t) \eta^* \phi_i^\eta \tag{16}$$

where $\phi_i^l =: \frac{\dot{l}_i}{l_i}$ and $\phi_i^\eta =: \frac{\dot{d}_i^\eta}{d_i^\eta}$ with $\dot{l}_i = {g^*}^\top \nu_i$ and $\dot{d}_i^\eta = a_i(t) {\eta^*}^\top v_i$, and

$$a_i(t) := \begin{cases} 1, \ {\eta^*}^\top p_i \leq \frac{w}{2}, \\ -1, \ \text{otherwise}. \end{cases} \tag{17}$$

V. Stability Analysis

Recalling (1), (12), (13), and (16), one verifies that the closed-loop dynamics of the error variable $(\tilde{p}_i, \tilde{v}_i), i \in \mathcal{V}/\{1\}$ can be rewritten as

$$\begin{cases} \dot{\tilde{p}}_i = \tilde{v}_i \\ \dot{\tilde{v}}_i = k_1 g^* {g^*}^\top (\tilde{e}_i + \nu_i) - k_2 \eta^* {\eta^*}^\top (\tilde{p}_i + \tilde{v}_i) + u_{i-1} - \dot{v}_i^* \\ \qquad + k_3 g^* \phi_i^l - k_4 a_i(t) \eta^* \phi_i^\eta \end{cases} \tag{18}$$

For the stability analysis of the proposed controller, we start with a single-follower scenario with the following lemma.

Lemma 2: Consider a 2-agent system with the dynamics (1) and let the input u_2 be given by (12) along with (13), and (16). If Assumptions 1-4 are satisfied, then for any initial conditions $(\tilde{p}_2(0), \tilde{v}_2(0))$ such that $l_2(0) > 0$, $d_2^\eta(0) > 0$, $\phi_2^l(0)$ and $\phi_2^\eta(0)$ are bounded, the following assertions hold $\forall t > 0$

1) d_2 and d_2^η remains positive, ϕ_2^l, ϕ_2^η and u_2 are bounded,

TABLE I: Initial vehicle states for the merging scenario

Vehicle	x_{ir} [m]	y_{ir} [m]	θ_i [rad]	v_{ir} [m/s]	δ_i [rad]
1	50	10	0	15	0
2	42.4	13.5	0	18	0
3	36	10	0	15	0
4	28.6	6	0	30	0
5	22	10	0	15	0

TABLE II: Initial vehicle states for the formation scenario

Vehicle	x_{ir} [m]	y_{ir} [m]	θ_i [rad]	v_{ir} [m/s]	δ_i [rad]
1	50	18	0	15	0
2	44	16	0.3	30	0
3	38	8	-0.4	15	0
4	31	5	0	25	0
5	25	18	0	15	0

2) the desired equilibrium point $(\tilde{p}_2, \tilde{v}_2) = (0, 0)$ is asymptotically stable.

The proof of this lemma is provided in Appendix A.

The stability analysis for a general n-vehicle ($n \geq 3$) platoon formation is provided by the following theorem.

Theorem 1: Consider an n-agent ($n \geq 3$) system with the dynamics (1) along with the feedback control law (12), (13), and (16). If Assumptions 1-4 holds, then for any bounded initial conditions $(\tilde{p}_i(0), \tilde{v}_i(0))$ such that $l_i(0) > 0$ and $d_i^{\eta}(0) > 0$, $\phi_i^l(0)$ and $\phi_i^{\eta}(0)$ are bounded, the following assertions hold $\forall i \in \mathcal{V}/\{1\}$, $\forall t \geq 0$:

1) $d_i(t)$ and $d_i^{\eta}(t)$ remains positive and $\phi_i^l(t)$, $\phi_i^{\eta}(t)$, and u_i are bounded,
2) the desired equilibrium point $(\tilde{p}_i, \tilde{v}_i) = (0, 0)$ is asymptotically stable.

The proof of this theorem is given in Appendix B.

VI. Simulation Results

To illustrate the effectiveness of the proposed feedback control method (12) in the context of multi-lane platoon formation, we have designed two simulation scenarios, as depicted in Fig. 4. These scenarios are referred to as (a) the merging scenario and (b) the formation scenario.

In both scenarios, a total of five vehicles are employed. The platoon leader, designated as $i = 1$, is initially positioned at coordinates $(x_{ir}, y_{ir}) = (50\text{m}, 10\text{m})$ for the merging scenario and $(x_{ir}, y_{ir}) = (50\text{m}, 18\text{m})$ for the formation scenario. It moves along the x-direction at a constant velocity of $v_{ir} = 15$ m/s. Additionally, both scenarios share several common parameters, including road width $w = 20$ m, vehicle length $L_i = 4$ m, vehicle safe distance $r = 5$ m, road safe distance $r_\eta = 1.2$ m, desired platoon speed $c_v = 15$ m/s, and desired platoon spacing, $c_i = 14$ m. The gains for the nominal and collision avoidance controllers are set as $k_1 = 2$, $k_2 = 2$, $k_3 = 4$, and $k_4 = 5$.

To illustrate the effectiveness of the proposed controller in managing the merging of vehicles into an existing platoon, the merging scenario has been designed. Here, vehicles 1, 3, and 5 initially assume positions conforming to the desired platoon formation. Vehicles 2 and 4, on the other hand, are tasked with merging into the platoon. Vehicle 2 merges from the left side, while vehicle 4 merges from the right side of the platoon as depicted in Fig. 4a. A summary of the exact initial states for all vehicles involved in this merging scenario can be found in Table I.

For the formation scenario as illustrated in Fig. 4b, all follower vehicles with $i \geq 2$ are randomly placed in safe initial positions. This setup allows us to evaluate the controller's performance in steering vehicles from different lanes into the desired platoon formation. A detailed overview of the initial states for all vehicles participating in the formation process is provided in Table II.

Analyzing the progression of the formation process in both scenarios, as displayed in Fig. 4, we observe that all vehicles smoothly converge to the desired formation. Both formation processes reach completion within a distance of 100 meters, starting from the safe initial conditions. This convergence to the desired platoon formation is further evidenced by examining the evolution of the absolute position error $||\tilde{p}_i(t)||$ and the absolute velocity error $||\tilde{v}_i(t)||$ for all followers $i \geq 2$ over time, as depicted in Fig. 5. Both $||\tilde{p}_i(t)||$ and $||\tilde{v}_i(t)||$ converge to zero within 8 seconds, marking the successful completion of the formation process.

To assess the safety aspect of the proposed method, we compare the simulation results with a baseline control strategy which takes the form of the nominal controller (13) without the collision avoidance component (16). In Fig. 6, we compare the time evolution of the safe distance $d_i(t)$ and $d_i^{\eta}(t)$ between the proposed safe formation controller and the baseline controller. In both scenarios, the proposed method effectively maintains the safe distance above zero at all times, signifying compliance with safety conditions. In contrast, the baseline controller caused collisions in both scenarios, as it fails to keep $d_4 > 0$ in the merging scenario Fig. 6a, and in the formation scenario Fig. 6b, it violates both $d_2^{\eta} > 0$ and $d_4 > 0$. A video of the simulations can be found at http://bit.ly/platoon_formation.

VII. Conclusions

In this paper, we have designed a safe platoon formation control using constructive barrier feedback. The method allows the vehicles to converge to the desired platoon formation while avoiding inter-vehicle collisions and violation of the road edges. We provide a theoretical analysis of the performance and safety properties of the proposed controller. Through simulation studies, we further validate the efficacy of the controller in both formation and merging scenarios. Compared with the baseline controller, the simulation results demonstrate the capability of the proposed method to safely control the vehicles into the desired platoon formation as long as the initial condition is safe. In future works, we aim to investigate the generalization of the method to handle

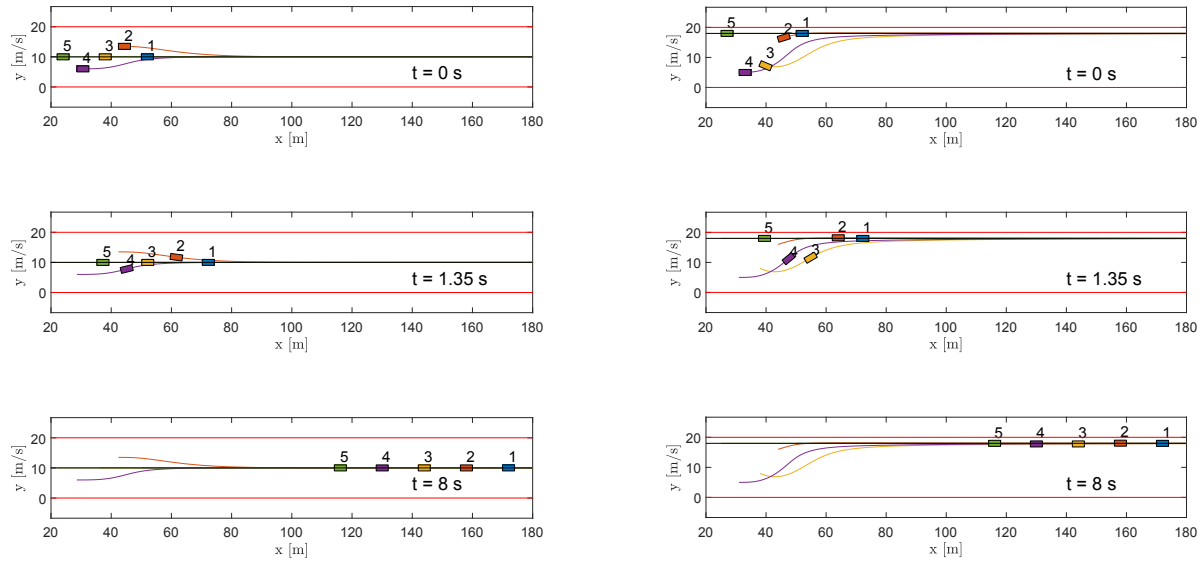

(a) The merging scenario.

(b) The formation scenario.

Fig. 4: Time evolution of the platoon formation process. Two parallel red solid lines are the road edges, the black solid line indicates the desired lane for the platoon, and the color solid lines indicate the vehicle trajectory during the formation process.

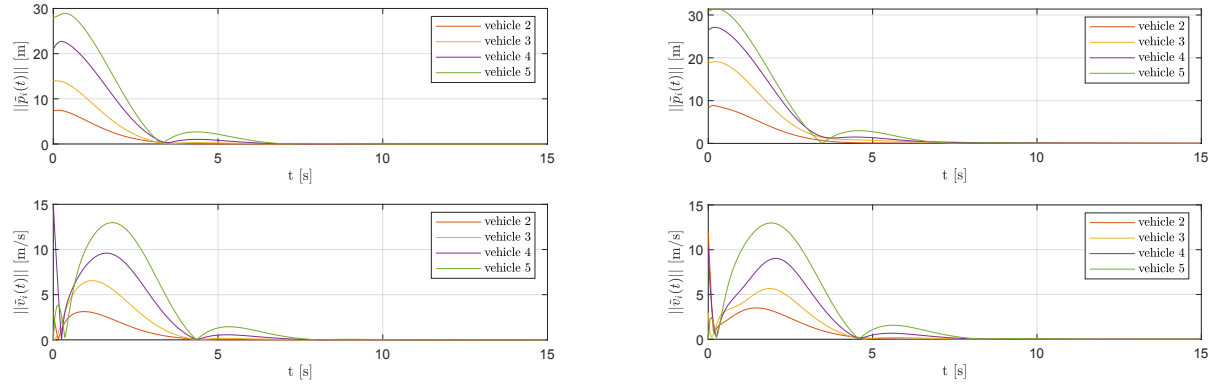

(a) The merging scenario

(b) The formation scenario

Fig. 5: Time evolution of the absolute position error $||\tilde{p}_i(t)||$ and the absolute velocity error $||\tilde{v}_i(t)||$ for all $i = \{2, 3, 4, 5\}$.

a broader class of traffic scenarios, including formation in curved roads and other types of graph topology. Another direction is to consider state and input constraints in the controller design and to handle model and measurement uncertainties with robustness.

APPENDIX

A. Proof of Lemma 2

Proof: Based on Assumption 3, we have $(p_1, v_1) = (p_1^*, v_1^*)$. Recall (18), the closed loop dynamics for the error variable $(\tilde{p}_2, \tilde{v}_2)$ of the follower vehicle 2 can then be simplified as:

$$\begin{cases} \dot{\tilde{p}}_2 = \tilde{v}_2 \\ \dot{\tilde{v}}_2 = -k_1 g^* g^{*\top}(\tilde{p}_2 + \tilde{v}_2) - k_2 \eta^* \eta^{*\top}(\tilde{p}_2 + \tilde{v}_2) \\ \qquad + k_3 g^* \phi_2^l - k_4 a_2(t) \eta^* \phi_2^\eta \end{cases} \tag{19}$$

Consider the following Lyapunov function candidate:

$$\mathcal{L}_2 = \frac{1}{2}\tilde{p}_2^\top K \tilde{p}_2 + \frac{1}{2}||\tilde{v}_2||^2 \tag{20}$$

where $K = \begin{bmatrix} k1I & 0 \\ 0 & k_2 I \end{bmatrix} > 0$. Differentiate $\mathcal{L}_2$, we get:

$$\dot{\mathcal{L}}_2 = -\tilde{v}_2^\top K \tilde{v}_2 + k_3 \tilde{v}_2^\top g^* \phi_2^l - k_4 a_2(t) \tilde{v}_2^\top \eta^* \phi_2^\eta \tag{21}$$

Recall that $\phi_2^l = \frac{l_2}{l_2}$, $\phi_2^\eta = \frac{d_2^\eta}{d_2^\eta}$ and use the fact that $\dot{l}_2 = g^{*\top}\nu_2 = -g^{*\top}\tilde{v}_2$, and $\dot{d}_{2\eta} = a_2(t)\eta^{*\top}v_2 = a_2(t)\eta^{*\top}\tilde{v}_2$,

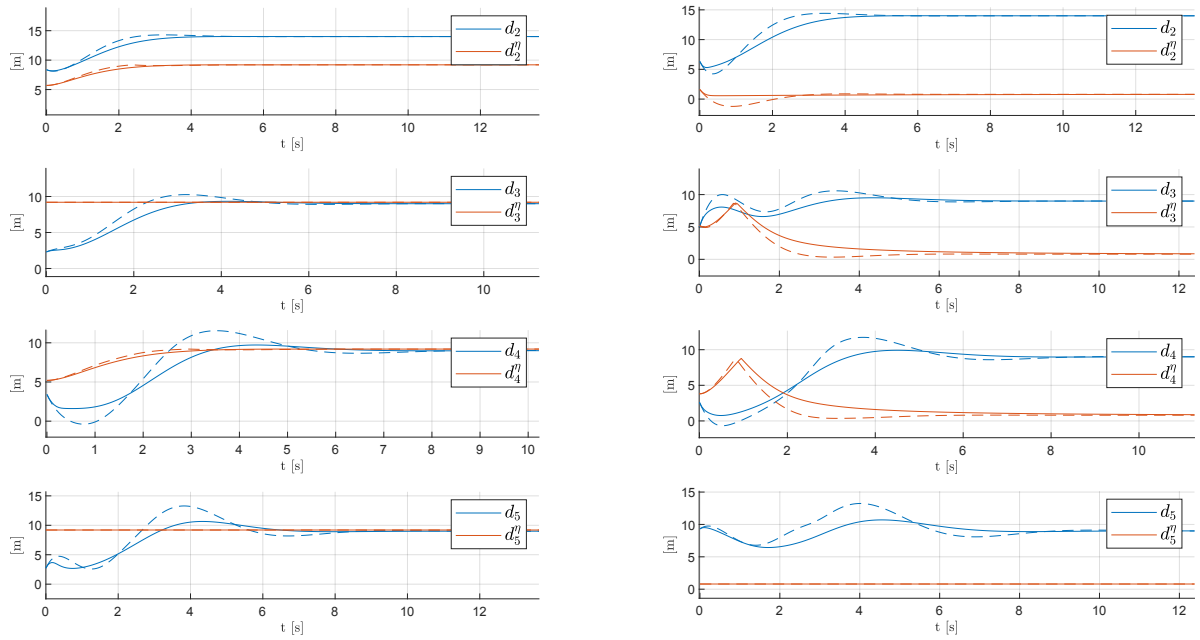

(a) Simulation result for the merging scenario

(b) Simulation result for the basic formation scenario

Fig. 6: Time evolution of the safe distance $d_i(t)$ and $d_i^\eta(t)$ for all $i \in \{2,3,4,5\}$. The solid lines indicate evolutions of $d_i(t)$ and $d_i^\eta(t)$ under the proposed controller (12), (13), and (16). The dashed lines indicate the result under only the baseline controller with nominal design (13).

$\dot{\mathcal{L}}_2$ can be simplified as

$$\dot{\mathcal{L}}_2 = -\tilde{v}_2^\top K \tilde{v}_2 - k_3 \frac{|\dot{l}_2|^2}{l_2} - k_4 \frac{|\dot{d}_2^\eta|^2}{d_2^\eta} \leq 0 \tag{22}$$

which is negative semi-definite provided $l_2 > 0$ and $d_2^\eta > 0$. This implies $(\tilde{p}_2, \tilde{v}_2)$ is bounded as long as l_2 and d_2^η remain positive.

Proof of item (1): Since $l_2 > 0$ implies $d_2 > 0$, we will prove $l_2 > 0$ in the following statement. Take the derivative of $\dot{l}_2 = {g^*}^\top \nu_2$ and $\dot{d}_2^\eta = a_2(t){\eta^*}^\top \tilde{v}_2$, due to the fact that ${g^*}^\top \eta^* = 0$, one has

$$\ddot{l}_2 = -k_3 \frac{\dot{l}_2}{l_2} + k_1 {g^*}^\top (\tilde{e}_2 + \nu_2) \tag{23a}$$

$$\ddot{d}_2^\eta = -k_4 \frac{\dot{d}_2^\eta}{d_2^\eta} - a_2(t) k_2 {\eta^*}^\top (\tilde{p}_2 + \tilde{v}_2). \tag{23b}$$

To prove that $l_2(t)$ and $d_2^\eta(t)$ will not approach zero in finite time, we use proof by contradiction. Assume there is a finite time $T > 0$ such that $l_2(T) = 0$ and $d_2^\eta(T) = 0$, taking the integral of (23) from 0 to T

$$\begin{aligned} k_3(\ln l_2(T) - \ln l_2(0)) &= \dot{l}_2(0) - \dot{l}_2(T) \\ &+ k_1 \int_0^T {g^*}^\top \tilde{e}_2 d\tau + k_1(l_2(T) - l_2(0)) \end{aligned} \tag{24a}$$

$$\begin{aligned} k_4(\ln d_2^\eta(t) - \ln d_2^\eta(0)) &= \dot{d}_2^\eta(0) - \dot{d}_2^\eta(t) \\ &- k_2 \int_0^T a_2(\tau) {\eta^*}^\top \tilde{p}_2 d\tau - k_2(d_2^\eta(t) - d_2^\eta(0)) \end{aligned} \tag{24b}$$

the left side of (24a) and (24b) tend to 'negative' infinity, while the right side of the corresponding equation is bounded or tends to 'positive' infinity, since ${g^*}^\top(\tilde{e}_2)$, $a_2(t){\eta^*}^\top(\tilde{p}_2)$ are bounded $\forall 0 < t < T$, and $\dot{l}_2(T)$, $\dot{d}_2^\eta(t)$ are either bounded or 'negative' infinity as l_2 and d_2^η approach to zero. This statement yields a contradiction. Hence, one concludes that l_2 (so does d_2) and d_2^η remain positive for all the time, which implies $(\tilde{p}_2, \tilde{v}_2)$ are bounded. A direct application of Lemma 1-item 3) concludes that ϕ_2^l and ϕ_2^η are bounded for all the time which implies u_2 is bounded for all the time.

Proof of Item (2): Using a similar argument as the proof of Lemma 2 - item (2) in [16], one concludes that the equilibrium point $(\tilde{p}_2, \tilde{v}_2) = (0,0)$ is asymptotically stable. The undesired equilibrium point described in [16, Lemma 2 - item (2)] does not appear here due to the Assumption 4. ■

B. Proof of theorem 1

Proof: We will proceed with the proof using mathematical induction. Since the case, $i = 2$ is equivalent to Lemma 2 and hence trivial, we will start by proving that the theory holds for $i = 3$.

Proof for $i = 3$: Recalling (18), the closed loop dynamics for $(\tilde{p}_3, \tilde{v}_3)$ is given as:

$$\begin{cases} \dot{\tilde{p}}_3 = \tilde{v}_3 \\ \dot{\tilde{v}}_3 = k_1 g^* {g^*}^\top (\tilde{e}_3 + \nu_3) - k_2 \eta^* {\eta^*}^\top (\tilde{p}_3 + \tilde{v}_3) \\ \qquad + u_2 - \dot{v}_3^* + k_3 g^* \phi_3^l - k_4 a_3(t) \eta^* \phi_3^\eta. \end{cases} \tag{25}$$

Since $\tilde{e}_3 = \tilde{p}_2 - \tilde{p}_3$ and $\nu_3 = \tilde{v}_2 - \tilde{v}_3$, (25) can be considered as a nominal system pertubered by $(\tilde{p}_2, \tilde{v}_2)$ to the unforced system

$$\begin{cases} \dot{\tilde{p}}_3 = \tilde{v}_3 \\ \dot{\tilde{v}}_3 = -k_1 g^* {g^*}^\top (\tilde{p}_3 + \tilde{v}_3) - k_2 \eta^* {\eta^*}^\top (\tilde{p}_3 + \tilde{v}_3) \\ \qquad + k_3 g^* \phi_3^l - k_4 a_3(t) \eta^* \phi_3^\eta \end{cases} \tag{26}$$

Consider a Lyapunov candidate for the unforced system (26):

$$\mathcal{L}_3 = \frac{1}{2} \tilde{p}_3^\top K \tilde{p}_3 + \frac{1}{2} ||\tilde{v}_3||^2. \tag{27}$$

Following the same argument as in the proof for Lemma 2, the derivative of $\mathcal{L}_3$ is obtained as:

$$\dot{\mathcal{L}}_3 = -\frac{1}{2} \tilde{v}_3^\top K \tilde{v}_3 - k_3 \frac{|\dot{l}_3|^2}{l_3} - k_4 \frac{|\dot{d}_3^\eta|^2}{d_3^\eta} \tag{28}$$

which is negative-semidefinite given that $l_3 > 0$ and $d_3^\eta > 0$.

Proof of item (1) for $i = 3$: Take the derivatives of $\dot{l}_3 = {g^*}^\top \nu_3$ and $\dot{d}_3^\eta = a_3(t) {\eta^*}^\top v_3$

$$\ddot{l}_3 = -k_3 \frac{\dot{l}_3}{l_3} - k_1 {g^*}^\top (\tilde{e}_3 + \nu_3) \tag{29a}$$

$$\ddot{d}_3^\eta = -k_4 \frac{\dot{d}_3^\eta}{d_3^\eta} - a_3(t) {\eta^*}^\top (k_2(\tilde{p}_3 + \tilde{v}_3) - u_2) \tag{29b}$$

Since u_2 is bounded as indicated in Lemma 2, one concludes that $\forall t \geq 0$, $l_3 > 0$ (hence, $d_3 > 0$), $d_3^\eta > 0$, ϕ_3^l, ϕ_3^η, and u_3 are bounded, using a similar argument as in the proof of Lemma 2 - item (1).

Proof of item (2) for $i = 3$: Using a similar argument as the proof of Lemma 2 - item (2), one concludes that the equilibrium point $(\tilde{p}_3, \tilde{v}_3) = (0, 0)$ of the unforced system (26) is asymptotically stable. Since $(\tilde{p}_2, \tilde{v}_2) = (0, 0)$ is asymptotically stable, one conclude that $(\tilde{p}_3, \tilde{v}_3) = (0, 0)$ of the nominal system (25) is also asymptotically stable.

Proof for $i \geq 4$: Now, assuming that the theorem is true for $i - 1 \geq 3$, using an analogous statement as for $i = 3$, one concludes that the theorem is also true for $i \geq 4$. By mathematical induction, we conclude that items 1 and 2 hold true for all agents $i \in \mathcal{V}/\{1\}$. ■

REFERENCES

[1] J. N. Bajpai, "Emerging vehicle technologies & the search for urban mobility solutions," *Urban, Planning and Transport Research*, vol. 4, no. 1, pp. 83–100, 2016.

[2] S. E. Shladover, X.-Y. Lu, B. Song, S. Dickey, C. Nowakowski, A. Howell, F. Bu, D. Marco, H.-S. Tan, and D. Nelson, "Demonstration of automated heavy-duty vehicles," 2006.

[3] M. Saeednia and M. Menendez, "Analysis of strategies for truck platooning: Hybrid strategy," *Transportation Research Record*, vol. 2547, no. 1, pp. 41–48, 2016.

[4] S. Bang and S. Ahn, "Platooning strategy for connected and autonomous vehicles: transition from light traffic," *Transportation Research Record*, vol. 2623, no. 1, pp. 73–81, 2017.

[5] V. Turri, B. Besselink, and K. H. Johansson, "Cooperative look-ahead control for fuel-efficient and safe heavy-duty vehicle platooning," *IEEE Transactions on Control Systems Technology*, vol. 25, no. 1, pp. 12–28, 2016.

[6] Y. Zheng, S. E. Li, J. Wang, D. Cao, and K. Li, "Stability and scalability of homogeneous vehicular platoon: Study on the influence of information flow topologies," *IEEE Transactions on intelligent transportation systems*, vol. 17, no. 1, pp. 14–26, 2015.

[7] L. Xiao and F. Gao, "Practical string stability of platoon of adaptive cruise control vehicles," *IEEE Transactions on intelligent transportation systems*, vol. 12, no. 4, pp. 1184–1194, 2011.

[8] Y. Li, C. Tang, S. Peeta, and Y. Wang, "Integral-sliding-mode braking control for a connected vehicle platoon: Theory and application," *IEEE Transactions on Industrial Electronics*, vol. 66, no. 6, pp. 4618–4628, 2018.

[9] E. Rimon, *Exact robot navigation using artificial potential functions*. Yale University, 1990.

[10] R. Olfati-Saber, "Flocking for multi-agent dynamic systems: Algorithms and theory," *IEEE Transactions on automatic control*, vol. 51, no. 3, pp. 401–420, 2006.

[11] Y. Liu and B. Xu, "Improved protocols and stability analysis for multivehicle cooperative autonomous systems," *IEEE Transactions on Intelligent Transportation Systems*, vol. 16, no. 5, pp. 2700–2710, 2015.

[12] H. Zheng, J. Wu, W. Wu, and R. R. Negenborn, "Cooperative distributed predictive control for collision-free vehicle platoons," *IET Intelligent Transport Systems*, vol. 13, no. 5, pp. 816–824, 2019.

[13] P. Liu, A. Kurt, and U. Ozguner, "Distributed model predictive control for cooperative and flexible vehicle platooning," *IEEE Transactions on Control Systems Technology*, vol. 27, no. 3, pp. 1115–1128, 2018.

[14] L. Wang, A. D. Ames, and M. Egerstedt, "Safety barrier certificates for collisions-free multirobot systems," *IEEE Transactions on Robotics*, vol. 33, no. 3, pp. 661–674, 2017.

[15] A. Frauenfelder, A. Wiltz, and D. V. Dimarogonas, "Decentralized vehicle coordination and lane switching without switching of controllers," *arXiv preprint arXiv:2305.04885*, 2023.

[16] Z. Tang, R. Cunha, T. Hamel, and C. Silvestre, "Constructive barrier feedback for collision avoidance in leader-follower formation control," in *2023 62nd IEEE Conference on Decision and Control (CDC)*. IEEE, 2023. [Online]. Available: https://arxiv.org/abs/2310.14258

[17] P. S. Bhagavatula, C. Claudianos, M. R. Ibbotson, and M. V. Srinivasan, "Optic flow cues guide flight in birds," *Current Biology*, vol. 21, no. 21, pp. 1794–1799, 2011.

[18] A. De Luca, G. Oriolo, and C. Samson, "Feedback control of a nonholonomic car-like robot," *Robot motion planning and control*, pp. 198–201, 2005.

[19] L. Rosa, T. Hamel, R. Mahony, and C. Samson, "Optical-flow based strategies for landing vtol uavs in cluttered environments," *IFAC Proceedings Volumes*, vol. 47, no. 3, pp. 3176–3183, 2014.

[20] M.-D. Hua and H. Rifaï, "Obstacle avoidance for teleoperated underactuated aerial vehicles using telemetric measurements," in *49th IEEE Conference on Decision and Control (CDC)*. IEEE, 2010, pp. 262–267.